

Chemically Etched Sharpened Tip of Transparent Crystallized Glass Fibers with Nonlinear Optical Ba₂TiSi₂O₈ Nanocrystals

Itaru ENOMOTO, Yasuhiko BENINO, Takumi FUJIWARA* and Takayuki KOMATSU

Department of Materials Science and Technology, Nagaoka University of Technology, 1603-1, Kamitomioka-cho, Nagaoka-shi 940-2188

*Department of Applied Physics, Graduate School of Engineering, Tohoku University, 6-6-05, Aoba, Sendai-shi 980-8579

Glass fibers with a diameter of $\sim 100 \mu\text{m}$ are drawn by just pulling up melts of $40\text{BaO} \cdot 20\text{TiO}_2 \cdot 40\text{SiO}_2$ glass, and transparent crystallized glass fibers consisting of nonlinear optical fresnoite Ba₂TiSi₂O₈ nanocrystals (particle size: $\sim 100\text{--}200 \text{ nm}$) are fabricated by crystallization of glass fibers. Precursor glass fibers and nanocrystallized glass fibers are etched chemically using a meniscus method, in which an etching solution of 0.1 wt% HF/hexane is used. Glass fibers with sharpened tips (e.g., the taper length is $\sim L = 200 \mu\text{m}$ and the tip angle is $\sim \theta = 23^\circ$) are obtained. It is found that etched nanocrystallized glass fibers also have sharpened tips ($L = 50 \mu\text{m}$, $\theta = 80^\circ$). Compared with precursor glass fibers, nanocrystallized glass fibers show a high resistance against chemical etching in a 0.1 wt% HF solution. Although sharpened tips in nanocrystallized glass fibers do not have nanoscaled apertures, the present study suggests that nanocrystallized glass fibers showing second harmonic generations would have a potential for fiber-type light control optical devices.

[Received April 5, 2007; Accepted May 17, 2007]

Key-words: Nanocrystal, Glass fiber, Chemical etching, Ba₂TiSi₂O₈, Second harmonic generation

1. Introduction

Nanostructures are the gateway into a new realm in physical, chemical, biological and materials science. Developing techniques with low costs for fabricating nanostructures is an area that requires substantial effort. Crystallization of glass is one of the effective methods for fabrication of nanostructures,¹⁾ and recently new optically transparent bulk nanocrystallized glasses (glass-ceramics) have been successfully fabricated in TeO₂-, GeO₂-, and SiO₂-based glasses.^{2)–6)} Among them, transparent nanocrystallized glasses consisting of nonlinear optical/ferroelectric nanocrystals have received much attention, and in particular, fibers with nonlinear optical nanocrystals are of interest,^{7)–9)} because such fibers are potential candidates for light control devices in fiber networks. For instance, Iwafuchi et al.⁸⁾ have reported nanocrystallized glass fibers with second harmonic generations (SHGs) in the K₂O–Nb₂O₅–TeO₂ system. Prasad et al.⁹⁾ have tried to fabricate TeO₂-based glass fibers containing nonlinear optical KNbO₃ crystals. It should be also pointed out that some studies on transparent crystallized glass fibers with transition metal doped nanocrystals, oxyfluoride nanocrystals, and sharpened tips have been reported.^{10)–12)}

In this study, we focus our attention on the fabrication of chemically etched sharpened tips of transparent crystallized glass fibers with nonlinear optical Ba₂TiSi₂O₈ nanocrystals. It is known that BaO–TiO₂–SiO₂ glasses show a prominent nanocrystallization and transparent nanocrystallized glasses consisting of nonlinear optical fresnoite Ba₂TiSi₂O₈ nanocrystals are fabricated.^{5),13),14)} However, there has been no report on fibers with Ba₂TiSi₂O₈ nanocrystals. A meniscus chemical etching method is applied for tip sharpenings of nanocrystallized glass fibers in the present study. Microfabrication of crystallized glass fibers such as tip sharpening would be needed for their device applications such as near-field fiber probes and photonic fibers, but such studies for crystallized glass fibers are scarce.¹²⁾

2. Experiments

The Glass composition examined in the present study is $40\text{BaO} \cdot 20\text{TiO}_2 \cdot 40\text{SiO}_2$ (mol%) (designated here as BTS), which corresponds to the stoichiometric composition of non-

linear optical Ba₂TiSi₂O₈ crystals. Commercial powders of reagent grade BaCO₃, TiO₂, and SiO₂ were mixed and melted in a platinum crucible at 1550°C for 1 h. Glass fibers with a diameter of $\sim 100 \mu\text{m}$ were prepared by pulling up melts using silica glass rods, where the pulling rate of silica rods is $\sim 1 \text{ m/s}$. In this method, fibers were prepared by a hand-operated technique, but not using any fiber drawing machines. The glass transition and crystallization peak temperatures of glass fibers were determined using differential thermal analyses (DTA) at a heating rate of 10 K/min.

The glass fibers were heat treated to obtain transparent nanocrystallized glass fibers, and the crystalline phase present in the heat-treated samples was examined by X-ray diffraction (XRD) analyses at room temperature using Cu K α radiation. Second harmonic generations (SHGs) of crystallized fibers were examined by measuring second harmonic waves (a wavelength of $\lambda = 532 \text{ nm}$) for the incident light of a Q-switched Nd: YAG laser with $\lambda = 1064 \text{ nm}$. Glass and nanocrystallized fibers were etched using a meniscus chemical etching method,¹⁵⁾ in which etching solutions such as 0.1 wt% HF/hexane were used. A schematic illustration for the meniscus etching method is shown in Fig. 1. In this etching technique, it is expected that the evolution of a meniscus at the interface between fiber and solution leads to the formation of sharpened tips, and hexane is used as a protecting overlayer against HF etching solutions.

3. Results

3.1 Fabrication of transparent nanocrystallized glass fibers

The optical micrographs for the glass fibers prepared are shown in Fig. 2. It is seen that the fiber shows a diameter of $\sim 100 \mu\text{m}$ and almost a perfect circle in the cross-section. The DTA patterns for bulk plate glasses and fibers are shown in Fig. 3, indicating almost the same patterns and thus the same values of glass transition, T_g , crystallization onset, T_x , and crystallization peak, T_p , temperatures. That is, BTS glass fibers have the values of $T_g = 728$, $T_x = 788$, and $T_p = 805^\circ\text{C}$.

The optical micrographs for the fibers obtained by heat treatments at 760, 780, and 800°C for 1 h are shown in Fig. 4. It is seen that all the heat-treated fibers keep a good trans-

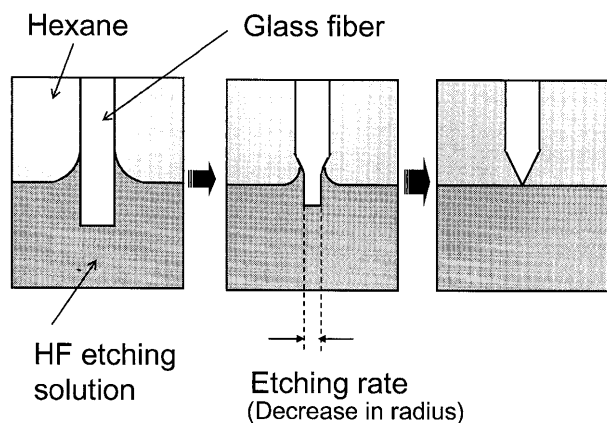


Fig. 1. Schematic illustration for the meniscus etching method. In this study, a solution of HF/hexane is used. The etching rate was estimated from the decrease in the radius of fiber.

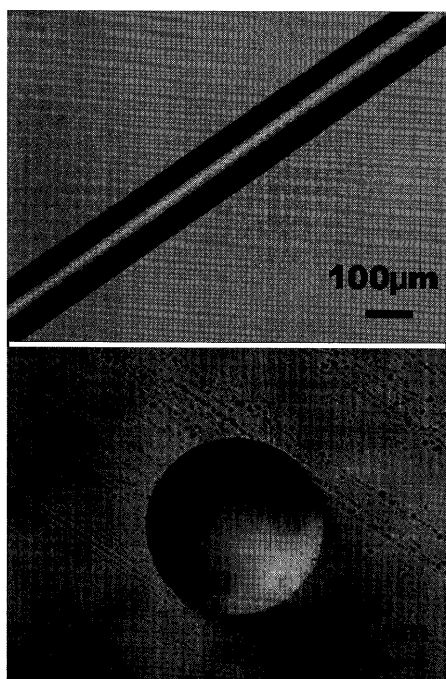


Fig. 2. Optical micrographs for the glass fiber prepared in this study. The glass composition is $40\text{BaO} \cdot 20\text{TiO}_2 \cdot 40\text{SiO}_2$.

parency. The powder XRD patterns for the samples obtained by the heat treatments are shown in Fig. 5. The XRD peaks are assigned to the $\text{Ba}_2\text{TiSi}_2\text{O}_8$ crystalline phase, indicating that fresnoite $\text{Ba}_2\text{TiSi}_2\text{O}_8$ crystals are formed even in the fibers as similar to the crystallization of bulk plate glasses.^{5),13),14)} The SHG microscope images¹⁶⁾ for the transparent crystallized glass fiber obtained by a heat treatment at 800°C for 1 h are shown in Fig. 6. The generation of second harmonic (SH) waves (green color) is clearly observed. For the sample obtained by a heat treatment at 780°C for 1 h, the SH waves with weak intensities were observed. As already reported by Takahashi et al.,^{5),13)} $\text{Ba}_2\text{TiSi}_2\text{O}_8$ nanocrystals with a diameter of 100–200 nm are easily formed by crystallization at temperatures of $720\text{--}800^\circ\text{C}$ in bulk BTS glasses. The results shown in Figs. 3 to 6 indicate, therefore, that nonlinear optical $\text{Ba}_2\text{TiSi}_2\text{O}_8$ crystals are formed even in the fibers as similar

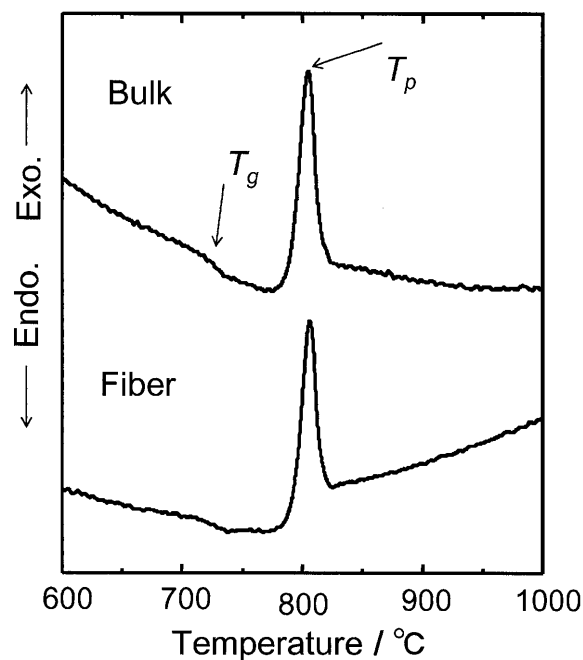


Fig. 3. DTA patterns for the bulk glass plate and fiber. Heating rate was 10 K/min. The glass composition is $40\text{BaO} \cdot 20\text{TiO}_2 \cdot 40\text{SiO}_2$.

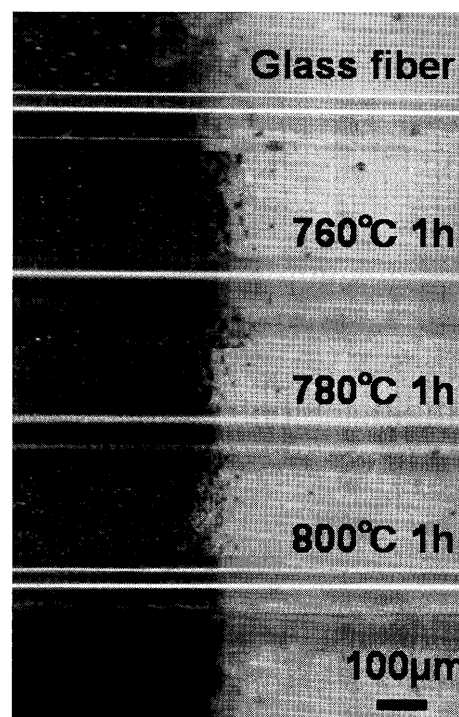


Fig. 4. Optical micrographs for the precursor glass fiber and crystallized glass fibers. The glass composition is $40\text{BaO} \cdot 20\text{TiO}_2 \cdot 40\text{SiO}_2$.

to bulk (plate-shape) BTS glasses.

3.2 Chemical etching of nanocrystallized glass fibers

Prior to studying nanocrystallized glass fibers, the etching behavior of precursor glass fibers was examined. The optical micrographs for the glass fiber samples obtained by a meniscus etching method with different HF concentrations in HF/

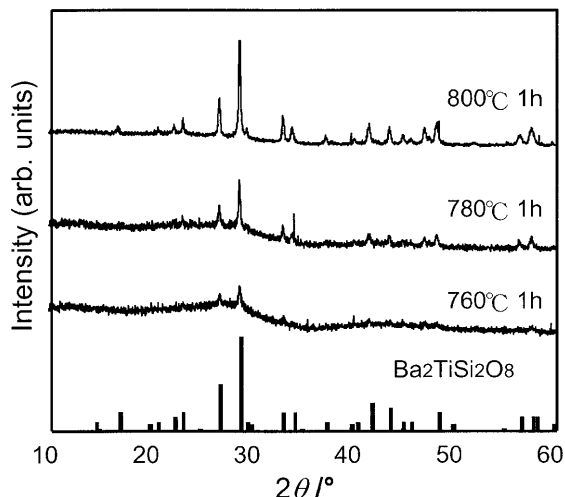


Fig. 5. Powder XRD patterns at room temperature for the crystallized fibers obtained by heat-treatments at 760, 780, and 800°C for 1 h. The crystalline phase formed in these fibers is $\text{Ba}_2\text{TiSi}_2\text{O}_8$. The glass composition is $40\text{BaO} \cdot 20\text{TiO}_2 \cdot 40\text{SiO}_2$.

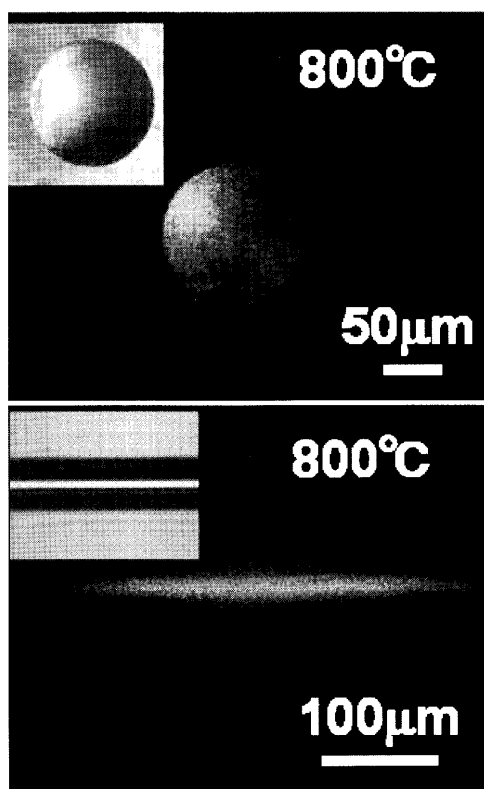


Fig. 6. SHG microscope images for the crystallized glass fibers obtained by a heat-treatment at 800°C for 1 h. The glass composition is $40\text{BaO} \cdot 20\text{TiO}_2 \cdot 40\text{SiO}_2$.

hexane etching solutions are shown in Fig. 7. The temperature of etching solutions was fixed to room temperature. It is seen that a solution of 20 wt% HF gives a rapid etching and a tapered tip can not be obtained. In a solution of 1 wt% HF, the etched surface is not smooth, probably some salts formed during the etching would adhere to the etched surface. In solutions of 0.5 and 0.25 wt% HF, more proper etchings occur and tapered tips are formed. The optical micrograph for the

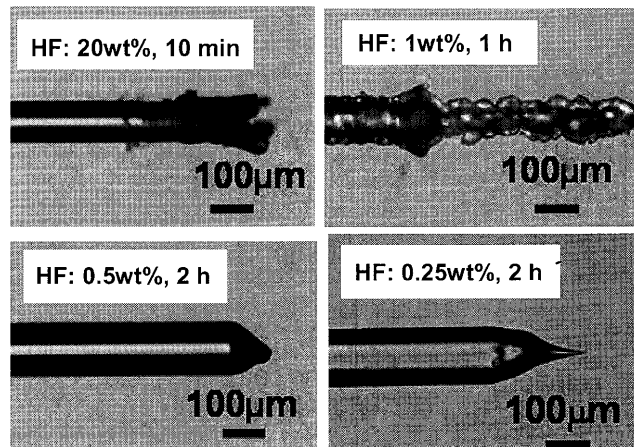


Fig. 7. Optical micrographs for the glass fiber samples obtained by a meniscus etching method with different HF concentrations in HF/hexane etching solutions. The etching temperature is room temperature. The glass composition is $40\text{BaO} \cdot 20\text{TiO}_2 \cdot 40\text{SiO}_2$.

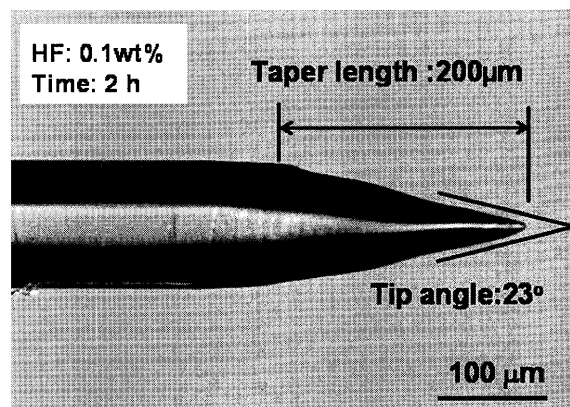


Fig. 8. Optical micrograph for the precursor glass fiber obtained by an etching with a solution of 0.1 wt% HF and for 2 h. The glass composition is $40\text{BaO} \cdot 20\text{TiO}_2 \cdot 40\text{SiO}_2$.

sample obtained by an etching with a solution of 0.1 wt% HF and for 2 h is shown in Fig. 8. It is seen that a sharpened tip with the taper length of 200 μm and the tip angle of 23° is formed. Although the tip (aperture size) does not show a nanoscaled size, the data shown in Fig. 8 demonstrate that the 0.1wt%-HF/hexane system works as a good etching solution for BTS glass fibers.

The optical micrograph for the nanocrystallized (780°C, 1 h) sample obtained by an etching with a solution of 0.1 wt% HF and for 2 h is shown in Fig. 9. It is clear that the meniscus etching method using a 0.1 wt%-HF/hexane solution system works well even for nanocrystallized glass fibers and a sharpened tip with the taper length of 50 μm and the tip angle of 80° is obtained. This result shown in Fig. 9 indicates that the etching behavior for nanocrystallized glass fibers is different from that for precursor glass fibers (Fig. 8).

The etching rate in a solution of 0.1 wt% HF at room temperature was estimated from the decrease in the radius of fibers, and the measuring position of etched fibers is shown schematically in Fig. 1. The data on the etching rate are shown in Fig. 10. The precursor glass fibers have an etching rate of $\sim 0.6 \mu\text{m}/\text{min}$. On the other hand, the nanocrystallized glass

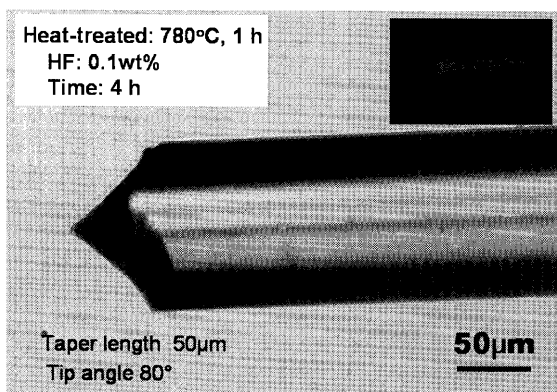


Fig. 9. Optical micrograph for the nanocrystallized (780°C, 1 h) sample obtained by an etching with a solution of 0.1 wt% HF and for 4 h. The glass composition is 40BaO·20TiO₂·40SiO₂.

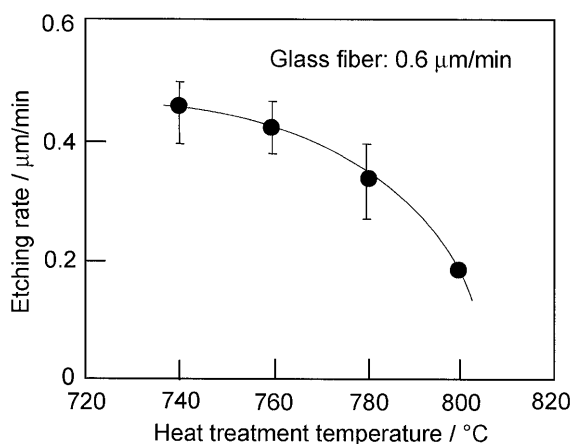


Fig. 10. Etching rates for the crystallized glass fibers obtained by heat-treatments at 760, 780, and 800°C for 1 h. The etching solution is 0.1 wt% HF/hexane and the etching time is 2 h. The glass composition is 40BaO·20TiO₂·40SiO₂.

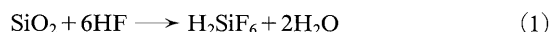
fibers have the etching rates of 0.18–0.46 µm/min. Furthermore, it is seen that the etching rate decreases with increasing heat treatment temperature.

4. Discussion

The nanocrystallization behavior of BTS (40BaO·20TiO₂·40SiO₂) bulk (not fiber) glasses has been studied in detail by Cabal et al.,¹³ and it has been reported that BTS glasses show extremely high nucleation rates. Furthermore, Takahashi et al.^{5),14} have reported that nanocrystallized glasses consisting of Ba₂TiSi₂O₈ nanocrystals show relatively strong SHGs. The present study demonstrates that BTS glass fibers also show a prominent nanocrystallization similar to BTS bulk glasses. Indeed, as shown in Fig. 6, SHGs have been detected even in nanocrystallized glass fibers. For practical applications, it is desired to examine the light transmission loss of BTS nanocrystallized glass fibers quantitatively, and such a study is now under consideration.

The chemical etching behavior of bulk SiO₂-based glasses in HF-based solutions has been extensively studied so far,^{17)–19)} and the following mechanism has been proposed:¹⁷⁾ reactive species of HF and HF₂⁻ and catalytic H⁺ ions are adsorbed first at the glass surface and then the breaking of ≡Si–O–Si≡

(siloxane) bonds in the silicate network occurs. The overall reaction is as follows;



In SiO₂ glass, it is necessary to break all four siloxane bonds to break down the network structure and release silicon atoms from the glass surface. The etching rate of SiO₂ glass in HF solutions increases rapidly with increasing HF content, and a solution of 5 wt% HF gives an etching rate of ~0.5 nm/s.¹⁹⁾ On the other hand, in SiO₂-based glasses with network modifiers such as Na₂O, K₂O and BaO, the etching rate in HF solutions increases largely, because network modifiers themselves are breaking partially siloxane bonds. For instance, the etching rate of 30Na₂O·70SiO₂ glass in a solution of 5 wt% HF at room temperature is ~20 nm/s.¹⁹⁾

As shown in Fig. 10, the etching rate of BTS glass (40BaO·20TiO₂·40SiO₂) in a solution of 0.1 wt% HF is 0.6 µm/min, i.e., 10 nm/s. As the BTS glass contains a large amount of BaO (network modifier) and consists of a small amount of SiO₂ (glass former), it is considered that such a high etching rate of 10 nm/min would be obtained. TiO₂ oxide has been recognized as intermediate for the glass formation, and the single bond strength of Ti–O bonds in TiO₂ is reported to be 305 kJ/mol. The single bond strengths of Si–O bonds in SiO₂ and Ba–O bonds in BaO are 443 and 138 kJ/mol, respectively.²⁰⁾ It is, therefore, considered that Ti–O bonds in BTS glass would play an intermediate role on the etching in HF solutions in comparison with BaO and SiO₂.

As can be seen in Fig. 10, the etching rate of BTS glass fibers decreases due to the nanocrystallization, i.e., the formation of Ba₂TiSi₂O₈ nanocrystals. For instance, the fibers obtained by a heat treatment at 800°C for 1 h show an etching rate of about 0.18 µm/min (3 nm/s). The nanocrystallized glass fibers consist of Ba₂TiSi₂O₈ nanocrystals, glassy phase, and grain boundaries between nanocrystals. Furthermore, the amount of the glassy phase would decrease significantly due to the nanocrystallization, because the glass composition of 40BaO·20TiO₂·40SiO₂ corresponds to the stoichiometric composition of Ba₂TiSi₂O₈ crystals and this glass shows a bulk (not surface) nanocrystallization. The density of the bulk (not fiber) nanocrystallized sample obtained by a heat treatment at 800°C for 1 h is $d = 4.39 \text{ g/cm}^3$. The volume fraction of Ba₂TiSi₂O₈ nanocrystals, f , in this sample was estimated from the following equation:

$$d = (1 - f)d(\text{glass}) + fd(\text{crystal}) \quad (2)$$

where $d(\text{glass})$ and $d(\text{crystal})$ are the densities of BTS glass ($d = 4.29 \text{ g/cm}^3$) and Ba₂TiSi₂O₈ crystals ($d = 4.43 \text{ g/cm}^3$). From Eq. (3), the volume fraction of the nanocrystallized (800°C, 1 h) sample is estimated to be $f = 0.7$. It is, therefore, considered that even in nanocrystallized (800°C, 1 h) glass fibers the volume fraction of Ba₂TiSi₂O₈ nanocrystals would be around 70%. The chemical durability of Ba₂TiSi₂O₈ crystal itself against HF solutions has not been examined. The results shown in Fig. 10, however, indicate that the composites of Ba₂TiSi₂O₈ nanocrystals and the glassy phase have stronger resistance against HF solutions in comparison with the BTS glassy phase itself.

In nanoscale science and technology, scanning near-field optical microscope (SNOM) absorbs great interests, in which usually optical SiO₂-based glass fiber probes with sharpened tips have been used.^{21)–23)} In the physics of near-field optics, the strength of near-field waves, E , generated at the surface of a nanoparticle is given by the following equation, when light with an electric field of E_0 is irradiated to a given nanoparticle

with an electronic polarizability of α ,

$$E = \frac{E_0\alpha}{4\pi\epsilon_0 r^3} \quad (3)$$

where ϵ_0 is a dielectric constant of vacuum, r is a distance for the position giving a near-field strength of E .²⁴⁾ Equation (3) means that the magnitude of E is proportional to the electric field strength of irradiated lights and to the dielectric constant of a given nanoparticle. It is well known that the dielectric constant of SiO₂ glass is around 4, which is an extremely small value among oxide glasses. Considering the physical concept for the generation of near field lights around the surface of particles, nanoparticles or sharpened tip fibers consisting of materials with high refractive indices (high dielectric constants) are favorable for near-field optical probes. In such materials, the generation of high intense near-field lights would be expected through the generation of electric dipoles under light irradiations.

The dielectric constants (1 kHz, room temperature), ϵ , of BTS glass and crystallized (heat-treated at 780°C for 1 h) glass (not fibers) were measured in this study, and the following values were obtained: $\epsilon=42$ for BTS glass and $\epsilon=45$ for the crystallized sample. These values obtained for bulk plate samples would be expected even for the precursor glass fibers and crystallized glass fibers with Ba₂TiSi₂O₈ nanocrystals fabricated in this study. It should be emphasized that these dielectric constants are much higher than that ($\epsilon=4$) for SiO₂ glass. Although fibers with well-sharpened (nanoscaled aperture) tips have not been fabricated in this study, the data shown in Figs. 8 to 10 give us important clues for further studies. Again, it should be emphasized that the present study on a chemical etching of nonlinear optical nanocrystallized glass fibers is the first challenge in this field. It is desired to examine the etching behavior of transparent nanocrystallized glass fibers in different etching solutions and to find optimal etching solutions and conditions for the fabrication of fibers with nanoscaled apertures.

5. Summary

The glass fibers with a diameter of $\sim 100 \mu\text{m}$ were drawn by just pulling out melts of 40BaO·20TiO₂·40SiO₂ glass, and transparent crystallized glass fibers consisting of nonlinear optical fresnoite Ba₂TiSi₂O₈ nanocrystals (particle size: ~ 100 – 200 nm) were fabricated by crystallization of glass fibers. The nanocrystallized glass fibers were etched chemically using a meniscus etching method, in which an etching solution of 0.1 wt% -HF/hexane was used. Nanocrystallized glass fibers with sharpened tips (e.g., the taper length is $\sim 50 \mu\text{m}$ and the tip angle is $\sim 80^\circ$) were obtained. Compared with precursor glass fibers, nanocrystallized glass fibers have a high resistance against chemical etchings. The present study suggests that nanocrystallized glass fibers would have a potential for fiber-type light control optical devices.

Acknowledgements This work was supported from the Grant-in-Aid for Scientific Research from the Ministry of Educa-

tion, Science, Sport, and Culture, Japan, and by the 21st Century Center of Excellence (COE) Program in Nagaoka University of Technology. The authors also would like to thank Hosokawa Powder Technology Foundation for the partial financial support to this work.

References

- 1) Beall, G. H. and Pinckney, L. R., *J. Am. Ceram. Soc.*, Vol. 82, pp. 5–16 (1999).
- 2) Shioya, K., Komatsu, T., Kim, H. G. and Matusita, K., *J. Non-Cryst. Solids*, Vol. 189, pp. 16–24 (1995).
- 3) Sakai, R., Benino, Y. and Komatsu, T., *Appl. Phys. Lett.*, Vol. 77, pp. 2188–2120 (2000).
- 4) Naito, K., Benino, Y., Fujiwara, T. and Komatsu, T., *Solids State Commun.*, Vol. 131, pp. 289–294 (2004).
- 5) Takahashi, Y., Kitamura, K., Benino, Y., Fujiwara, T. and Komatsu, T., *Appl. Phys. Lett.*, Vol. 86, pp. 091110/1–091110/3 (2005).
- 6) Torres, F., Narita, K., Benino, Y., Fujiwara, T. and Komatsu, T., *J. Appl. Phys.*, Vol. 94, pp. 5265–5272 (2003).
- 7) Kim, H. G., Komatsu, T., Sato, R. and Matusita, K., *J. Ceram. Soc. Japan.*, Vol. 103, pp. 1073–1076 (1995).
- 8) Iwafuchi, N., Mizuno, S., Benino, Y., Fujiwara, T., Komatsu, T., Koide, M. and Matusita, K., *Adv. Mater. Res.*, Vol. 11–12, pp. 209–212 (2006).
- 9) Prasad, N. S., Wang, J., Pattnaik, R. K., Jain, H. and Toukouse, J., *J. Non-Cryst. Solids*, Vol. 352, pp. 519–523 (2006).
- 10) Tick, P. A., Borrelli, N. F. and Reaney, I. M., *Opt. Mater.*, Vol. 15, pp. 81–91 (2000).
- 11) Samson, B. N., Pinckney, L. R., Wang, J., Beall, B. H. and Borrelli, N. F., *Opt. Lett.*, Vol. 27, pp. 1309–1311 (2002).
- 12) Enomoto, I., Benino, Y. Y., Fujiwara, T. and Komatsu, T., *J. Solid State Chem.*, Vol. 179, pp. 1821–1829 (2006).
- 13) Cabral, A. A., Fokin, V. M., Zanotto, E. D. and Chinaglia, C. R., *J. Non-Cryst. Solids*, Vol. 330, pp. 174–186 (2003).
- 14) Takahashi, Y., Kitamura, K., Inoue, S., Benino, Y., Fujiwara, T. and Komatsu, T., *J. Ceram. Soc. Japan.*, Vol. 113, pp. 419–423 (2005).
- 15) Turner, D. R., "Etch procedure for optical fibers," U.S. Patent, Vol. 4469, pp. 554 (1983).
- 16) Fujiwara, T., Sawada, T., Honma, T., Benino, Y., Komatsu, T., Takahashi, M., Yoko, T. and Nishii, J., *Jpn. J. Appl. Phys.*, Vol. 42, pp. 7326–7330 (2003).
- 17) Boksay, Z. and Bouquest, G., *Phys. Chem. Glasses*, Vol. 21, pp. 110–113 (1980).
- 18) Spierings, G.A.C.M., *J. Mater. Sci.*, Vol. 26, pp. 3329–3336 (1991).
- 19) Spierings, G.A.C.M., *J. Mater. Sci.*, Vol. 28, pp. 6261–6273 (1993).
- 20) Sun, K. H., *J. Am. Ceram. Soc.*, Vol. 30, pp. 277–281 (1947).
- 21) Monomobe, S., Naya, M., Saiki, T. and Ohtsu, *Appl. Opt.*, Vol. 36, pp. 1496–1500 (1997).
- 22) Sayah, A., Philipona, C., Lambelet, P., Pfeffer, M. and Marquis-Weible, F., *Ultramicroscopy*, Vol. 71, pp. 59–63 (1998).
- 23) Micheletto, R., Yoshimatsu, N. and Okazaki, S., *Opt. Commun.*, Vol. 188, pp. 11–15 (2001).
- 24) Ohtsu, M. and Kobayashi, K., *Basis of Near-Field Light* (in Japanese), Ohmsha, Tokyo, 2003, pp. 74, 93.